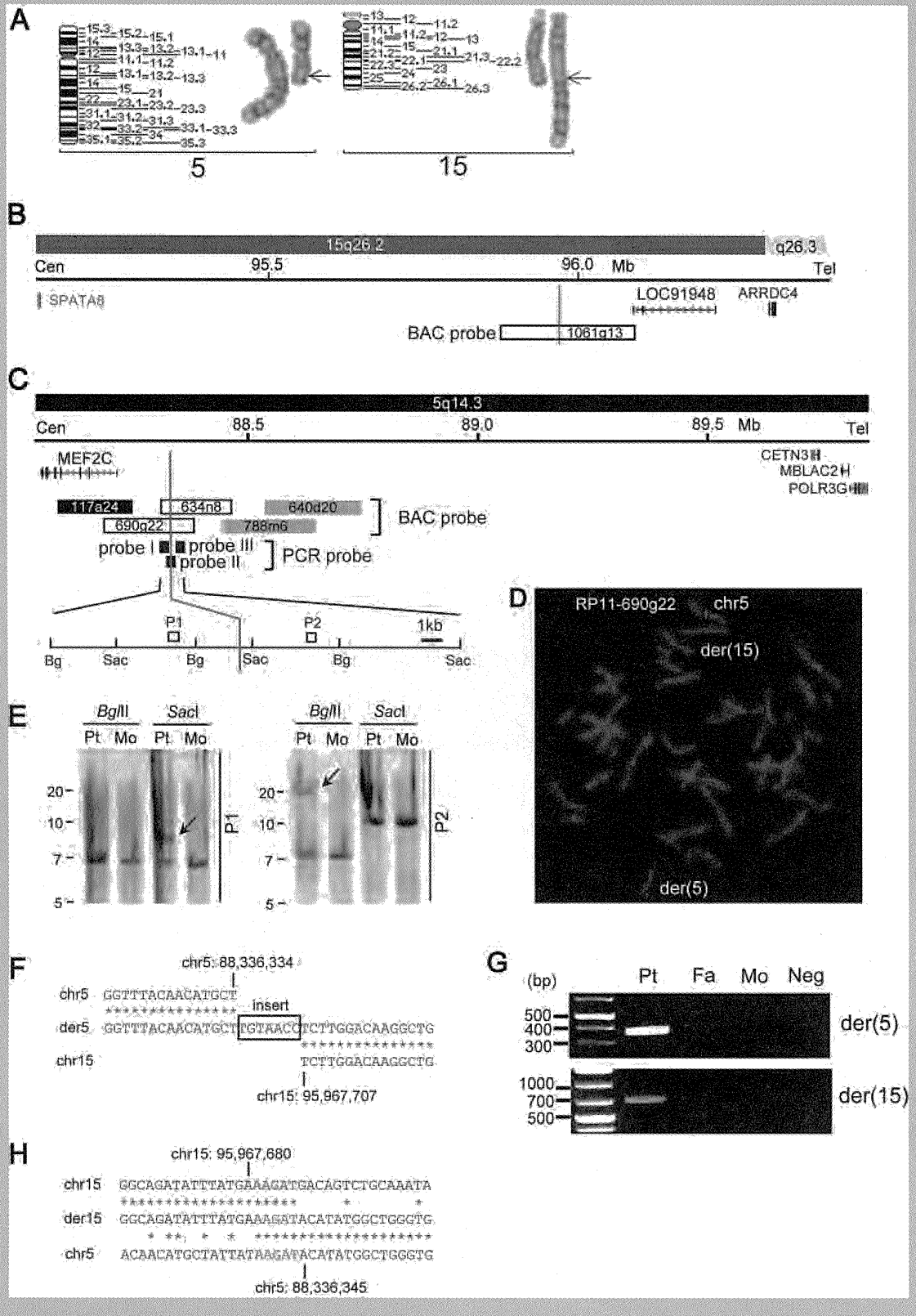
A
5
15
B
15q26.2
q26.3
Cen
95.5
96.0 Mb
Tel
SPATA8
LOC91948
ARRDC4
BAC probe
1061g13
C
5q14.3
Cen
88.5
89.0
89.5 Mb
Tel
MEF2C
CETN3
MBLAC2
POLR3G
117a24
634n8
640d20
690g22
788m6
BAC probe
probe I
probe III
probe II
PCR probe
P1
P2
1kb
Bg
Sac
Bg
Sac
Bg
Sac
D
RP11-690g22
chr5
der(15)
der(5)
E
BglII
SacI
Pt
Mo
Pt
Mo
BglII
SacI
Pt
Mo
Pt
Mo
20
10
7
5
P1
20
10
7
5
P2
F
chr5: 88,336,334
chr5 GGTTTACAACATGCT
insert
der5 GGTTTACAACATGCTTGTAACCTCTTGGACAAGGCTG
chr15 TCTTGGACAAGGCTG
chr15: 95,967,707
G
(bp)
Pt
Fa
Mo
Neg
500
400
300
der(5)
1000
700
500
der(15)
H
chr15: 95,967,680
chr15 GGCAGATATTTATGAAAGATGACAGTCTGCAAATA
der15 GGCAGATATTTATGAAAGATACATATGGCTGGGTG
chr5 ACAACATGCTATTATAAGATACATATGGCTGGGTG
chr5: 88,336,345

FIG. 2.

15q26.2 breakpoint was determined at the nucleotide level by sequencing of the beakpoint-specific PCR fragment (Fig. 1H). It was located 119-kb downstream of *LOC91948* non-coding RNA (Fig. 2B). To check genomic copy number alterations accompanied by the rearrangement, Cytogenetics Whole-Genome 2.7M Array (Affymetrix, Santa Clara, CA) was performed. Besides five known copy number variations, no other imbalances were detected (data not shown).

DISCUSSION

Expression of the members of MEF2 family transcription factors (*MEFA-D*) in the developing brain, which belong to the MADS (MCMl-agamous-deficiens-serum response factor) superfamily of DNA-binding proteins, shows spaciotemporal patterns correlating with withdrawal from the cell cycle and initiation of neuronal differentiation [Lyons et al., 1995]. After mouse *Mef2c* is first expressed in developing brain at embryonic day 11.5, *Mef2c* is highly expressed in cerebral cortex, hippocampus, amygdala, thalamus, midbrain, and Purukinje cells in the adult brain [Lyons et al., 1995]. It has recently reported that two independent conditional knockout lines of *Mef2c*, which resulted in deletion of *Mef2c* in neural stem/progenitor cells (NSCs), showed significant neurological deficits. One line with deletion of *Mef2c* in NSCs later in development showed impairment of hippocampal-dependent learning and memory, suggesting that *Mef2c* can limt excessive synapse formation during activity-dependent refinement of synaptic connectivity [Barbosa et al., 2008]. Of note, deletion of *Mef2c* in NSCs earlier in development resulted in severe behavioral deficits reminiscent of Rett syndrome [Li et al., 2008]. The mice also exhibited fewer, smaller, and more compacted neurons, similar to findings in Rett syndrome [Li et al., 2008]. In humans, *MEF2C* mutation/deletion cause severe ID, epilepsy, hypotonia, and cerebral malformations [Engels et al., 2009; Le Meur et al., 2010; Novara et al., 2010; Nowakowska et al., 2010; Zweier et al., 2010]. In addition, some patients showed repetitive clapping movements like Rett syndrome [Le Meur et al., 2010]. Considering essential roles of *MEF2C* in brain development both in humans and mice, the precise control of *MEF2C* expression should be very important.

In our patient, the 5q14.3 breakpoint was located 121.5-kb upstream of *MEF2C*. Two previous reports suggested that genomic regions 233- to 500-kb upstream of *MEF2C* may be required for proper *MEF2C* expression: a 3.57-Mb microdeletion 233.3-kb upstream of *MEF2C* resulted in significant loss of *MEF2C* expression [Zweier et al., 2010], and a de novo balanced translocation located approximately 500-kb upstream of *MEF2C* was associated with ID, epilepsy, and stereotypic movements similar to *MEF2C* mutation/deletion [Floris et al., 2008]. Thus, it is likely that the translocation may disrupt regulation of *MEF2C* expression in the developing brain. However, we did not observe any significant decrease of *MEF2C* expression in lymphoblastoide cells derived from the patient (data not shown). It has been reported that *MEF2C* expression in blood cells was significantly decreased in all patients with either a microdeletion or a truncating mutation [Zweier et al., 2010]. We speculate that the 5q14.3 translocation may alter proper *MEF2C* expression in the developing brain of the patient analyzed here.

The patient showed severe ID, early-onset epileptic encephalopathy. Brain MRI showed hypoplastic corpus callosum, especially in genu and splenium. All the three features (severe ID, seizure, and cerebral malformation) are common in patients with the *MEF2C* mutation/deletion. By contrast, our patient showed spastic quadriplegia, but not muscluar hypotonia which is common in approximately 90% of patients with *MEF2C* mutation/deletion (19/21) [Engels et al., 2009; Le Meur et al., 2010; Novara et al., 2010; Nowakowska et al., 2010; Zweier et al., 2010]. Thus, our patient may be an atypical case of *MEF2C* abnormality, probably due to unusual *MEF2C* expression in the brain caused by the 5q14.3 translocation.

In conclusion, we described a patient with severe ID, early-onset epileptic encephalopathy, and hypoplastic corpus callosum, carrying a de novo reciprocal translocation 121.5-kb upstream of *MEF2C*. Our report strengthens the role of *MEF2C* in severe ID with early-onset epileptic encephalopathy, and highlights importance of its upstream regulatory region.

FIG. 2. Genomic characterization of t(5;15)(q13.3;q26.1). A: Partial karyotype of the patient. Left shows chromosomes 5 (left: normal, right: derivative), and right shows chromosomes 15 (left: normal, right: derivative). B,C: Summarized physical maps covering the 15q26.2 (B) and 5q14.3 (C) translocation breakpoints. RP11-1061g13 spans the 15q26.2 breakpoint (B, red longitudinal line). RP11-690g22 and 634n8, and PCR probe II span the 5q14.3 breakpoint (C, red line). Note that the translocation did not directly disrupt any genes. More detailed maps are shown (C, bottom). A partial restriction map (Bg, *Bgl*II; Sac, *Sac*I), probes for Southern hybridization (P1, P2) are indicated. Translocation breakpoint (red line) is located between P1 and P2. D: FISH analysis using RP11-690g22 as a probe showed signals on chromosome 5, and der(5) and der(15) chromosomes. E: Southern hybridization using probes P1, and P2 on genomic DNA of the patient and her mother. Arrow shows aberrant bands specific to the patient (not observed in maternal DNA). Pt, patient; Mo, mother. F: Breakpoint junction sequences of der(5). Top, middle, and bottom sequence strands show normal 5, derivative 5, and normal 15 chromosomes, respectively. Breakpoint positions are marked with small longitudinal lines based on the UCSC genome browser coordinates (version March 2006). Asterisks indicate nucleotides identical to normal chromosomes. A small 7-bp nucleotide insertion was identified at the breakpoint (box). G: Breakpoint-specific PCR analysis of the patient's family. Primers specific to der(5) and der(15) breakpoints could successfully amplify 366- and 689-bp products, respectively, only from the patient (Pt), indicating the translocation occurred de novo. Fa, father; Mo, mother. H: Breakpoint junction sequences of der(15). Top, middle, and bottom sequence strands show normal 15, derivative 15, and normal 5 chromosomes, respectively. The five overlapping nucleotides (colored in red) are identified at the breakpoint.

ACKNOWLEDGMENTS

We would like to thank the patient and her family for their participation in this study. This work was supported by Research Grants from the Ministry of Health, Labour and Welfare (H.S., N. Matsumoto, N. Miyake, and M.K.), Grant-in-Aid for Scientific Research from Japan Society for the Promotion of Science (N. Matsumoto, N. Miyake and M.K.), Grant-in-Aid for Young Scientist from Japan Society for the Promotion of Science (H.S. and N. Miyake), Research Promotion Fund from Yokohama Foundation for Advancement of Medical Science (H.S.), Research Grants from the Japan Epilepsy Research Foundation (H.S. and M.K.), and Research Grant from Naito Foundation (N. Matsumoto).

REFERENCES

Barbosa AC, Kim MS, Ertunc M, Adachi M, Nelson ED, McAnally J, Richardson JA, Kavalali ET, Monteggia LM, Bassel-Duby R, Olson EN. 2008. MEF2C, a transcription factor that facilitates learning and memory by negative regulation of synapse numbers and function. Proc Natl Acad Sci USA 105:9391–9396.

Cardoso C, Boys A, Parrini E, Mignon-Ravix C, McMahon JM, Khantane S, Bertini E, Pallesi E, Missirian C, Zuffardi O, Novara F, Villard L, Giglio S, Chabrol B, Slater HR, Moncla A, Scheffer IE, Guerrini R. 2009. Periventricular heterotopia, mental retardation, and epilepsy associated with 5q14.3-q15 deletion. Neurology 72:784–792.

Claes L, Del-Favero J, Ceulemans B, Lagae L, Van Broeckhoven C, De Jonghe P. 2001. De novo mutations in the sodium-channel gene SCN1A cause severe myoclonic epilepsy of infancy. Am J Hum Genet 68: 1327–1332.

Engels H, Wohlleber E, Zink A, Hoyer J, Ludwig KU, Brockschmidt FF, Wieczorek D, Moog U, Hellmann-Mersch B, Weber RG, Willatt L, Kreiss-Nachtsheim M, Firth HV, Rauch A. 2009. A novel microdeletion syndrome involving 5q14.3-q15: Clinical and molecular cytogenetic characterization of three patients. Eur J Hum Genet 17:1592–1599.

Floris C, Rassu S, Boccone L, Gasperini D, Cao A, Crisponi L. 2008. Two patients with balanced translocations and autistic disorder: CSMD3 as a candidate gene for autism found in their common 8q23 breakpoint area. Eur J Hum Genet 16:696–704.

Holland KD, Hallinan BE. 2010. What causes epileptic encephalopathy in infancy?: The answer may lie in our genes. Neurology 75:1132–1133.

Kalscheuer VM, Tao J, Donnelly A, Hollway G, Schwinger E, Kubart S, Menzel C, Hoeltzenbein M, Tommerup N, Eyre H, Harbord M, Haan E, Sutherland GR, Ropers HH, Gecz J. 2003. Disruption of the serine/threonine kinase 9 gene causes severe X-linked infantile spasms and mental retardation. Am J Hum Genet 72:1401–1411.

Kato M, Saitoh S, Kamei A, Shiraishi H, Ueda Y, Akasaka M, Tohyama J, Akasaka N, Hayasaka K. 2007. A longer polyalanine expansion mutation in the ARX gene causes early infantile epileptic encephalopathy with suppression-burst pattern (Ohtahara syndrome). Am J Hum Genet 81: 361–366.

Le Meur N, Holder-Espinasse M, Jaillard S, Goldenberg A, Joriot S, Amati-Bonneau P, Guichet A, Barth M, Charollais A, Journel H, Auvin S, Boucher C, Kerckaert JP, David V, Manouvrier-Hanu S, Saugier-Veber P, Frebourg T, Dubourg C, Andrieux J, Bonneau D. 2010. MEF2C haploinsufficiency caused by either microdeletion of the 5q14.3 region or mutation is responsible for severe mental retardation with stereotypic movements, epilepsy and/or cerebral malformations. J Med Genet 47:22–29.

Li H, Radford JC, Ragusa MJ, Shea KL, McKercher SR, Zaremba JD, Soussou W, Nie Z, Kang YJ, Nakanishi N, Okamoto S, Roberts AJ, Schwarz JJ, Lipton SA. 2008. Transcription factor MEF2C influences neural stem/progenitor cell differentiation and maturation in vivo. Proc Natl Acad Sci USA 105:9397–9402.

Lyons GE, Micales BK, Schwarz J, Martin JF, Olson EN. 1995. Expression of mef2 genes in the mouse central nervous system suggests a role in neuronal maturation. J Neurosci 15:5727–5738.

Molinari F, Raas-Rothschild A, Rio M, Fiermonte G, Encha-Razavi F, Palmieri L, Palmieri F, Ben-Neriah Z, Kadhom N, Vekemans M, Attie-Bitach T, Munnich A, Rustin P, Colleaux L. 2005. Impaired mitochondrial glutamate transport in autosomal recessive neonatal myoclonic epilepsy. Am J Hum Genet 76:334–339.

Novara F, Beri S, Giorda R, Ortibus E, Nageshappa S, Darra F, Dalla Bernardina B, Zuffardi O, Van Esch H. 2010. Refining the phenotype associated with MEF2C haploinsufficiency. Clin Genet 78:471–477.

Nowakowska BA, Obersztyn E, Szymanska K, Bekiesinska-Figatowska M, Xia Z, Ricks CB, Bocian E, Stockton DW, Szczaluba K, Nawara M, Patel A, Scott DA, Cheung SW, Bohan TP, Stankiewicz P. 2010. Severe mental retardation, seizures, and hypotonia due to deletions of MEF2C. Am J Med Genet Part B 153B:1042–1051.

Saitsu H, Kato M, Mizuguchi T, Hamada K, Osaka H, Tohyama J, Uruno K, Kumada S, Nishiyama K, Nishimura A, Okada I, Yoshimura Y, Hirai S, Kumada T, Hayasaka K, Fukuda A, Ogata K, Matsumoto N. 2008. De novo mutations in the gene encoding STXBP1 (MUNC18-1) cause early infantile epileptic encephalopathy. Nat Genet 40:782–788.

Stromme P, Mangelsdorf ME, Shaw MA, Lower KM, Lewis SM, Bruyere H, Lutcherath V, Gedeon AK, Wallace RH, Scheffer IE, Turner G, Partington M, Frints SG, Fryns JP, Sutherland GR, Mulley JC, Gecz J. 2002. Mutations in the human ortholog of Aristaless cause X-linked mental retardation and epilepsy. Nat Genet 30:441–445.

Zweier M, Gregor A, Zweier C, Engels H, Sticht H, Wohlleber E, Bijlsma EK, Holder SE, Zenker M, Rossier E, Grasshoff U, Johnson DS, Robertson L, Firth HV, Ekici AB, Reis A, Rauch A. 2010. Mutations in MEF2C from the 5q14.3q15 microdeletion syndrome region are a frequent cause of severe mental retardation and diminish MECP2 and CDKL5 expression. Hum Mutat 31:722–733.

Journal of Human Genetics (2011) 56, 104–105

www.nature.com/jhg

COMMENTARY

Going BAC or oligo microarray to the well: A commentary on Clinical application of array-based comparative genomic hybridization by two-stage screening for 536 patients with mental retardation and multiple congenital anomalies

Mitsuhiro Kato

Journal of Human Genetics (2011) **56**, 104–105; doi:10.1038/jhg.2010.168; published online 13 January 2011

In this issue of the *Journal of Human Genetics*, Hayashi *et al.* document the results of their originally designed study of a 'two-stage screening' method that uses array-based comparative genomic hybridization for diagnosing patients who present with both multiple congenital anomalies and mental retardation (MCA/MR).[1] They collected DNA samples from 536 patients with MCA/MR by multicenter cooperation throughout Japan (from Hokkaido to Okinawa). They first screened all samples using the 'MCG Genome Disorder Array,' which covers subtelomeric regions and well-known disease-causing regions using 550 or 660 bacterial artificial chromosome (BAC)-based arrays that were originally constructed by them. Next, samples that did not show copy number variation (CNV) in the first stage of screening were screened again using 'MCG Whole Genome Array-4500,' which minutely covers all human chromosomes using 4523 bacterial artificial chromosomes at intervals of 0.7 Mb. In the first stage of screening, 54 (10.1%) patients showed CNVs that were confirmed by fluorescence *in situ* hybridization. In the second stage of screening, 63 (18.0%) of 349 patients demonstrated CNVs, of which 60 cases were confirmed by fluorescence *in situ* hybridization.

Dr M Kato is at the Department of Pediatrics, Yamagata University Faculty of Medicine, 2-2-2 Iida-nishi, Yamagata 990-9585, Japan.
E-mail: mkato@med.id.yamagata-u.ac.jp

The authors classified CNVs found in the second stage of screening into three categories: pathogenic, benign or variant of uncertain clinical significance). Initially, pathogenic CNVs were classified according to the following six criteria: (1) CNVs identified in recently established syndromes; (2) CNVs containing pathogenic gene(s); (3) recurrent CNVs in the same regions; (4) CNVs reported as pathogenic in previous studies; (5) large/gene-rich CNVs or CNVs containing morbid OMIM genes; or (6) *de novo* CNVs or CNVs that are maternally inherited through the X chromosome. CNVs that did not meet any of these criteria were classified as benign if they were inherited from a parent or as a variant of uncertain clinical significance if parental samples were not available. Consequently, 48 (13.8%) of 349 patients had pathogenic CNVs, 9 (2.6%) had benign CNVs and 6 (1.7%) had a variant of uncertain clinical significance.

MR is a highly heterogeneous condition and nearly 2500 syndromes of various congenital abnormalities are associated with MR[2] (http://becomerich.lab.u-ryukyu.ac.jp/). It is very difficult to determine the etiology of MR unless characteristic combinations of features can be accurately described, such as upslanted palpebral fissures in Down syndrome, overgrowth in Sotos syndrome, overeating in Prader–Willi syndrome or stereotypical hand movements in Rett syndrome, or unless specific and abnormal findings on laboratory or neuroimaging examinations are found, such as a metabolic screening indicative of phenylketonuria or lysosomal diseases, or brain magnetic resonance imaging indicative of polymicrogyria or lissencephaly. G-banded karyotyping has also been used to diagnose specific syndromes in patients with MCA/MR, and fluorescence *in situ* hybridizationis also useful for detecting microdeletion or microduplication syndromes; however, it is not easy for general practitioners or even pediatric neurologists to diagnose rare syndromes, such as Potocki–Lupski syndrome (17p11.2 duplication syndrome), Smith–Magenis syndrome (17p11.2 deletion syndrome) or 1p36 deletion syndrome. On the other hand, clinical applications of chromosomal microarrays are rapidly increasing for the diagnosis of congenital anomalies, hematological and solid tumors, and neuropsychological disorders, including MR and autism. In particular, chromosomal microarrays are used to diagnose MCA/MR. The diagnostic yields of chromosomal microarrays for detecting chromosomal aberrations among patients with MCA/MR or MR are only 7–15% in patients with normal G-banded karyotyping, depending on the probe coverage. These yields are much higher than G-banded karyotyping, which shows a yield of less than 3% if Down syndrome and other recognizable chromosomal syndromes are excluded.[3] The International Standard Cytogenomic Array Consortium and other groups support the consensus that chromosomal microarray is a first-tier clinical

diagnostic test and should be used before routine G-banded karyotyping for diagnosing individuals with unexplained developmental disabilities and/or congenital anomalies.[3–5] The 'two-stage screening' method by Hayashi *et al.* shows a diagnostic yield of 10.1% for the first targeted array and 13.8% for the second array capable of analyzing the whole genome. The total yield of their study was at least 18.1% (97 of 536 cases), which is comparable to the recent reports on higher-resolution oligonucleotide arrays. Unfortunately, G-banded karyotyping is still the first diagnostic tool for diagnosing MCA/MR in Japan because public health insurance currently covers only G-banded karyotyping and fluorescence *in situ* hybridization tests. Although chromosomal microarrays are much more expensive than G-banded cytogenetic analysis, the cost has reduced and is now less than the total cost of both traditional tests.[3] Thus, we now stand at the crossroads of genetic testing.

The study by Hayashi *et al.* used bacterial artificial chromosome-based arrays, while the expanded commercial availability of high-density oligonucleotide and single-nucleotide polymorphism arrays facilitates their use. In addition to good resolution, oligonucleotide arrays can detect regions of loss of heterozygosity and uniparental disomy (UPD), which are clinically important for the diagnosis of Silver–Russell syndrome and Beckwith–Wiedemann syndrome. Although major diseases caused by loss of heterozygosity or UPD, such as Prader–Willi syndrome and Angelman syndrome, can be clinically suspected by their characteristic features and UPD, most chromosomes show no phenotypic effects.[6] Physicians should know the limitations of each microarray in order to prevent the misdiagnosis of unfamiliar but important UPD disorders, such as maternal or paternal UPD chromosome 14.[7]

G-banded cytogenetic analysis still has the advantage over microarrays in terms of cost and ability to identify balanced rearrangements. Recognizable chromosomal syndromes, such as Down syndrome, trisomy 13, Turner syndrome, Klinefelter syndrome and MCA/MR with a family history of recurrent miscarriage or reproductive loss, all of which may be caused by balanced translocations, can be more efficiently diagnosed by traditional karyotyping.[3]

The application of microarrays to clinical testing is widening the scope of genomic medicine. Microarrays have accelerated the discovery of new syndromes and the causative genes of sporadic diseases, such as epileptic syndromes[8,9] and highly complex neuropsychological diseases.[10] However, the increasing number of variant of uncertain clinical significance cases makes definitive diagnosis difficult. No matter how far the tools for genetic analysis progress, clinical diagnosis based on medical history and examinations will remain pivotal. Future collaborations between basic scientists and trained clinicians, like the one performed in the study by Hayashi *et al.*,[1] will help to advance this new field.

1 Hayashi, S., Imoto, I., Aizu, Y., Okamoto, N., Mizuno, S., Kurosawa, K. *et al.* Clinical application of array-based comparative genomic hybridization by two-stage screening for 536 patients with mental retardation and multiple congenital anomalies. *J. Hum. Genet.* **56,** 110–124 (2011).
2 Naritomi, K. (UR-DBMS (University of the Ryukyus-Database for Malformation Syndromes), 2010) (http://becomerich.lab.u-ryukyu.ac.jp/).
3 Miller, D. T., Adam, M. P., Aradhya, S., Biesecker, L. G., Brothman, A. R., Carter, N. P. *et al.* Consensus statement: chromosomal microarray is a first-tier clinical diagnostic test for individuals with developmental disabilities or congenital anomalies. *Am. J. Hum. Genet.* **86,** 749–764 (2010).
4 Hochstenbach, R., van Binsbergen, E., Engelen, J., Nieuwint, A., Polstra, A., Poddighe, P. *et al.* Array analysis and karyotyping: workflow consequences based on a retrospective study of 36 325 patients with idiopathic developmental delay in the Netherlands. *Eur. J. Med. Genet.* **52,** 161–169 (2009).
5 Sagoo, G. S., Butterworth, A. S., Sanderson, S., Shaw-Smith, C., Higgins, J. P. & Burton, H. Array CGH in patients with learning disability (mental retardation) and congenital anomalies: updated systematic review and meta-analysis of 19 studies and 13 926 subjects. *Genet. Med.* **11,** 139–146 (2009).
6 Dawson, A., Chernos, J., McGowan-Jordan, J., Lavoie, J., Shetty, S., Steinraths, M. *et al.* CCMG guidelines: prenatal and postnatal diagnostic testing for uniparental disomy. *Clin. Genet.* (e-pub ahead of print 16 September 2010; doi:10.1111/j.1399-0004.2010.01547.x) (2010).
7 Hosoki, K., Kagami, M., Tanaka, T., Kubota, M., Kurosawa, K., Kato, M. *et al.* Maternal uniparental disomy 14 syndrome demonstrates Prader-Willi syndrome-like phenotype. *J. Pediatr.* **155,** 900–903 e901 (2009).
8 Saitsu, H., Kato, M., Mizuguchi, T., Hamada, K., Osaka, H., Tohyama, J. *et al. De novo* mutations in the gene encoding STXBP1 (MUNC18-1) cause early infantile epileptic encephalopathy. *Nat. Genet.* **40,** 782–788 (2008).
9 Saitsu, H., Tohyama, J., Kumada, T., Egawa, K., Hamada, K., Okada, I. *et al.* Dominant-negative mutations in alpha-II spectrin cause West syndrome with severe cerebral hypomyelination, spastic quadriplegia, and developmental delay. *Am. J. Hum. Genet.* **86,** 881–891 (2010).
10 Sebat, J., Lakshmi, B., Malhotra, D., Troge, J., Lese-Martin, C., Walsh, T. *et al.* Strong association of *de novo* copy number mutations with autism. *Science* **316,** 445–449 (2007).

Journal of Child Neurology
26(7) 885-890

DOI: 10.1177/0883073810393307
http://jcn.sagepub.com
SAGE

Acquired Opercular Epilepsy With Oromotor Dysfunction: Magnetoencephalographic Analysis and Efficacy of Corticosteroid Therapy

Jun Tohyama, MD[1], Noriyuki Akasaka, MD[1], Tsukasa Ohashi, MD, PhD[1], and Yu Kobayashi, MD[1]

Abstract

The authors describe herein the magnetoencephalographic findings and long-term outcome of a girl with acquired opercular epilepsy with oromotor dysfunction. She presented with brief episodes of unconsciousness, tremulous movements of the upper limbs, and negative myoclonus, in addition to convulsive seizures. She also had prolonged episodes of dysarthria and oral motor dysfunction, a gradual decrease in speech output, impairment of finger movements, and deterioration in cognitive performance over several years. Her electroencephalography (EEG) recordings showed notable continuous sharp or sharp-slow discharges during sleep. Brain magnetic resonance images revealed no structural anomalies. Magnetoencephalographic analysis showed broadly distributed epileptic foci around the sylvian fissure, including a secondary source, explaining the specific prolonged neurological dysfunction. Antiepileptic drugs could control her seizures; however, they did not improve the other neurological symptoms or epileptiform discharge on EEG. Administration of low-dose prednisolone over a long period was effective for improving the neurological impairments of this patient.

Keywords

acquired opercular epilepsy, oromotor dysfunction, magnetoencephalograpy, corticosteroid, Landau-Kleffner syndrome

Received September 26, 2010. Accepted for publication November 14, 2010.

Electrical status epilepticus during sleep is characterized by the presence of spike-and-wave discharges in at least 85% of non-rapid eye movement sleep.[1,2] A variety of neurocognitive impairments and regressions have been associated with this electroencephalography (EEG) pattern, including Landau-Kleffner syndrome and epilepsy with continuous spikes and waves during sleep.[3] A spike-wave index of 85% to 100% is considered too stringent as an EEG measure of electrical status epilepticus during sleep, and the definition of EEG showing "significant activation of epileptiform discharges by sleep" is widely accepted.[2] Acquired epileptiform opercular syndrome is a newly proposed epileptic syndrome that was first reported by Shafrir and Prensky in 1995.[4] This condition is characterized by acquired and prolonged oro-facial-lingual dysfunction with dysarthria, which resembles opercular syndrome, in association with electrical status epilepticus during sleep. Landau-Kleffner syndrome is characterized by acquired epileptiform aphasia during childhood, whereas acquired epileptiform opercular syndrome manifests as acquired motor impairment during childhood. Shafrir and Prensky speculated that this peculiar type of epilepsy is a distinct epileptic syndrome, equivalent to the Landau-Kleffner syndrome.[4] The pathophysiological mechanism of acquired opercular epilepsy is still not well understood. In Landau-Kleffner syndrome, various treatments have been used, including the administration of antiepileptics, corticosteroid, or intravenous immunoglobulin, and multiple subpial intracortical transections.[3] In contrast, only antiepileptics and ketogenic diet have been reported for the treatment of acquired opercular epilepsy.[4-7]

We report on magnetoencephalographic findings for evaluating the pathophysiology of acquired opercular epilepsy, and the long-term outcome of a girl with this condition who was successfully treated with corticosteroid.

[1] Department of Pediatrics, Epilepsy Center, Nishi-Niigata Chuo National Hospital, Niigata, Japan

Corresponding Author:
Jun Tohyama, MD, Department of Pediatrics, Epilepsy Center, Nishi-Niigata Chuo National Hospital, 1-14-1 Masago, Nishi-ku, Niigata 950-2085, Japan
Email: jtohyama@masa.go.jp

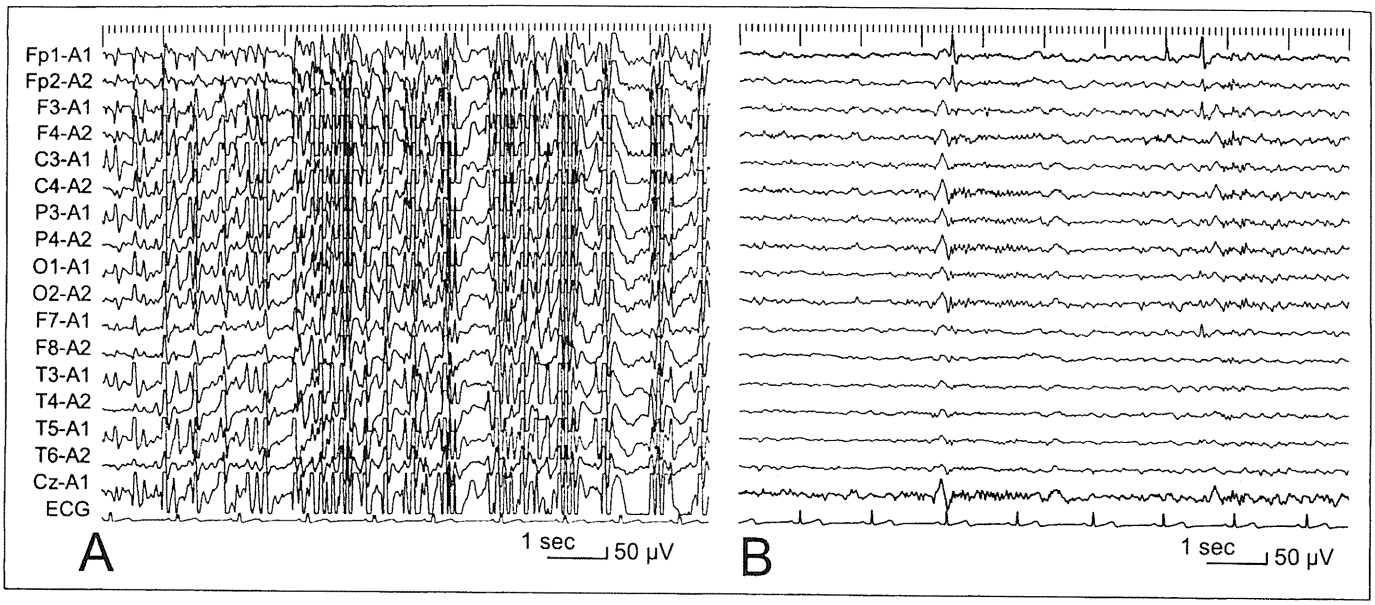

Figure 1. (A) Electroencephalography (EEG) recordings at the age of 9 years 9 months showed frequent and continuous sharp or sharp-slow discharges during sleep. The sharp wave amplitude exceeded 500 μV. (B) EEG at 16 years showed few sharp waves over the bilateral front polar and occipital regions during sleep.

Case Report

A girl, the first child of healthy nonconsanguineous parents, was born at 38 weeks gestation by normal vaginal delivery following an uneventful pregnancy. Her mother had suffered from epilepsy during childhood and had received antiepileptic medication for several years. Her birth weight was 3280 g, length was 50 cm, and occipitofrontal head circumference was 33 cm; her 3 younger brothers are healthy. She achieved normal developmental milestones during infancy, eg, she started to speak in single words at the age of 12 months and was able to walk alone at the age of 14 months. At the age of 5 years, she experienced her first episode of generalized convulsions during sleep. Soon after the first episode, she had another seizure. She was diagnosed with benign childhood epilepsy with centrotemporal spikes based on electroencephalographic findings at the referring hospital. Despite starting carbamazepine, she experienced several focal motor seizures involving the right arm and leg. At age 7 years 1 month, she developed tremulous movements of the right arm, causing difficulty in drawing and writing. Clonazepam was accordingly started and convulsive seizures improved thereafter. At age 7 years 3 months, she developed difficulty in handling a spoon or toothbrush. Around the same time, her parents noticed a gradual decrease in speech output, poor pronunciation, and deterioration in calculating performance. At age 7 years 4 months, she was referred to our hospital for an evaluation of her symptoms.

General physical examination revealed no abnormalities. We observed negative myoclonus in addition to tremulous movements of the upper limbs during action. Diadochokinesia was poor, but the cerebellar sign was not evident. Her facial appearance, eye movements, hearing, and gag reflex were normal. She could not follow any command or imitate movements involving her mouth and tongue, but no focal paresis was observed. At this point, the negative myoclonus and oral motor dysfunction increased. At age 7 years 6 months, she also developed brief episodes of unconsciousness with upward ocular deviation for a few seconds and was accordingly admitted to our hospital.

On admission, she had a slightly ataxic gait and slurred speech. She could not eat meals unaided. She experienced drooling and tended to retain food in her mouth. Brain magnetic resonance imaging (MRI) was normal. In terms of laboratory investigations, results of blood, serum, plasma, and urine studies were normal with respect to amino acids, organic acids, lactate, pyruvate, and ammonia. Cerebrospinal fluid proteins and glucose concentrations were also normal. Chromosome G-band analysis revealed a normal karyotype. Her intelligent quotient was 64 on the Wechsler Intelligence Scale for Children-Third Edition. After starting ethosuximide, the negative myoclonus and brief seizures involving loss of consciousness disappeared. Oral prednisolone therapy (2 mg/kg/d) was started at age 7 years 9 months. Her symptoms improved slightly, and prednisolone was quickly tapered. At age 9 years 6 months, she again showed a decrease in speech output, dysarthria, drooling, worsening of fine finger movements, and continuous drooling. EEG revealed an increase in frequency of the sharp and sharp-slow discharges during sleep, indicating electrical status (Figure 1A). The amplitude of sharp waves exceeded 500 μV. At age 9 years 9 months, she was treated with high-dose intravenous corticosteroid therapy (20 mg/kg methylprednisolone sodium succinate daily for 3 consecutive days). Prednisolone (1 mg/kg/d) was then given orally for 2 weeks before being gradually tapered. As the dose of prednisolone was tapered, the symptoms fluctuated; they sometimes increased when the dose was minimally reduced

Table 1. Chronological Summary of Electroencephalographic Findings and Antiepileptic Drug Treatment

Age, y, mo	EEG	AED	Efficacy
5 y	Rolandic spike	CBZ	No effect
6 y 10 mo	C4, P4, O2 spike, SWC	CBZ, VPA	No effect
7 y 1 mo		CBZ, VPA, CZP	CZP effective
7 y 4 mo	DS, SWC, predominantly left	CBZ, CZP, ZNS, PHT	ZNS, PHT not effective
7 y 6 mo	DS, SWC, predominantly left	CZP, ESM	ESM effective
7 y 9 mo	DS, SWC, both hemispheres	CZP, ESM, PSL	PSL partially effective
8 y	DS, SWC, both hemispheres	CZP, ESM, CLB	CLB not effective
8 y 4 mo	ESES	CZP, ESM, CLB, ACTH	ACTH not effective
9 y 9 mo	ESES	CZP, ESM, PSL	PSL effective
9 y 10 mo		CZP, ESM, PSL, DZP	DZP inconclusive
16 y 1 mo	Fp1, Fp2 sharp	CZP, ESM, DZP	

Abbreviations: EEG, electroencephalogram; SWC, spike and wave complex; DS, diffuse sharp; ESES, electrical status epileptics during sleep; AED, antiepileptic drug; CBZ, carbamazepine; VPA, valproic acid; CZP, clonazepam; ZNS, zonisamide; PHT, phenytoin; ESM, ethosuximide; PSL, prednisolone; CLB, clobazam; ACTH, adrenocorticotrophic hormonal; DZP, diazepam.

(to 0.12 mg/kg/d), and sometimes improved when the dose was increased. Low-dose prednisolone (0.12 ~ 0.5 mg/kg/d) was accordingly continued and adjusted for more than 5 years, corresponding to her neurological impairment. No serious side effects were observed. At age 16 years she demonstrated no dysarthria or oral motor deficit, and prednisolone was stopped. An EEG at this point showed a few sharp waves over the bilateral front polar and occipital region during sleep (Figure 1B). After terminating corticosteroid therapy, she experienced no relapse of neurological symptoms. Her electroencephalographic findings and antiepileptic drug treatment are summarized in chronological order in Table 1.

Magnetoencephalographic Analysis

Magnetoencephalography recording was performed using a helmet-shaped whole-scalp neuromagnetometer (Neuromag 204; Elekta-Neuromag, Oy, Finland) comprising 204 planar-type gradiometers in a magnetically shielded room at Nishi-Niigata-Chuo National Hospital. Before recording, the positions of 3 anatomical fiducial points (corresponding to the nasion and bilateral preauricular points) and 4 indicator coils on the scalp were digitized using a 3-dimensional electromagnetic digitizer (Polhems, Colchester, Vermont, USA). Magnetoencephalographic data were recorded for ≥20 minutes, then analyzed using a band-pass filter of 3 to 45 Hz. In magnetoencephalographic analysis, an equivalent current dipole was calculated for the initial peak of each interictal spike discharge in a spherical model. Equivalent current dipoles with a goodness of fit >80% and physiologically realistic current magnitude (Q < 500 nA) were accepted and superimposed onto T1-weighted 3-dimensional brain MRIs of the patient's brain using a 1.5-Tesla system (MAGNEX EPIOS 15; Shimadzu, Kyoto, Japan). EEG was simultaneously recorded.

The first magnetoencephalographic recordings were obtained at age 7 years 7 months, before the introduction of ethosuximide. Epileptic discharges were found in both hemispheres independently, or synchronously in the bilateral hemispheres, predominantly the left. Current dipoles of the left hemisphere were localized in the prerolandic area, presumably indicating the premotor cortex. Current dipoles of the right hemisphere were localized around the central sulcus and sylvian fissure (Figure 2A-2C). The second magnetoencephalographic recording was obtained at age 8 years 8 months, before starting the second course of corticosteroid therapy. High-amplitude epileptic discharges were observed bilaterally and synchronously, and some spikes were found independently in both hemispheres, predominantly the left. Current sources of left-sided discharges and right-sided discharges were distributed in a broad region surrounding the sylvian fissure, particularly in the superior temporal gyri and sensory cortex (Figure 2D-2F). Many equivalent current dipoles had a current magnitude exceeding 500 nA and were excluded in these analyses.

Discussion

The present patient was initially diagnosed with benign childhood epilepsy with centrotemporal spikes; however, she later developed brief episodes of unconsciousness, tremulous movements of the upper limbs, and negative myoclonus. She also demonstrated prolonged episodes of dysarthria and oral motor dysfunction, a gradual decrease in speech output, impairment of finger movements, and deterioration in school performance. Although her clinical seizures were well controlled, the neurological abnormalities fluctuated for several years. EEG showed continuous epileptiform activities for many years, despite anticonvulsant therapy. We considered that her diagnosis was acquired opercular epilepsy with oromotor dysfunction. This epileptic disorder was first proposed by Shafrir and Prensky[4] as a condition equivalent to the Landau-Kleffner syndrome. The opercular syndrome in children is usually caused by bilateral structural lesions in the anterior opercular area.[8] Shafrir and Prensky postulated that the epileptic opercular syndrome in children without any structural abnormality could be classified into ictal and nonictal (paraictal) phenomena.[4] Their patient presented with a paraictal syndrome, and they stated that the

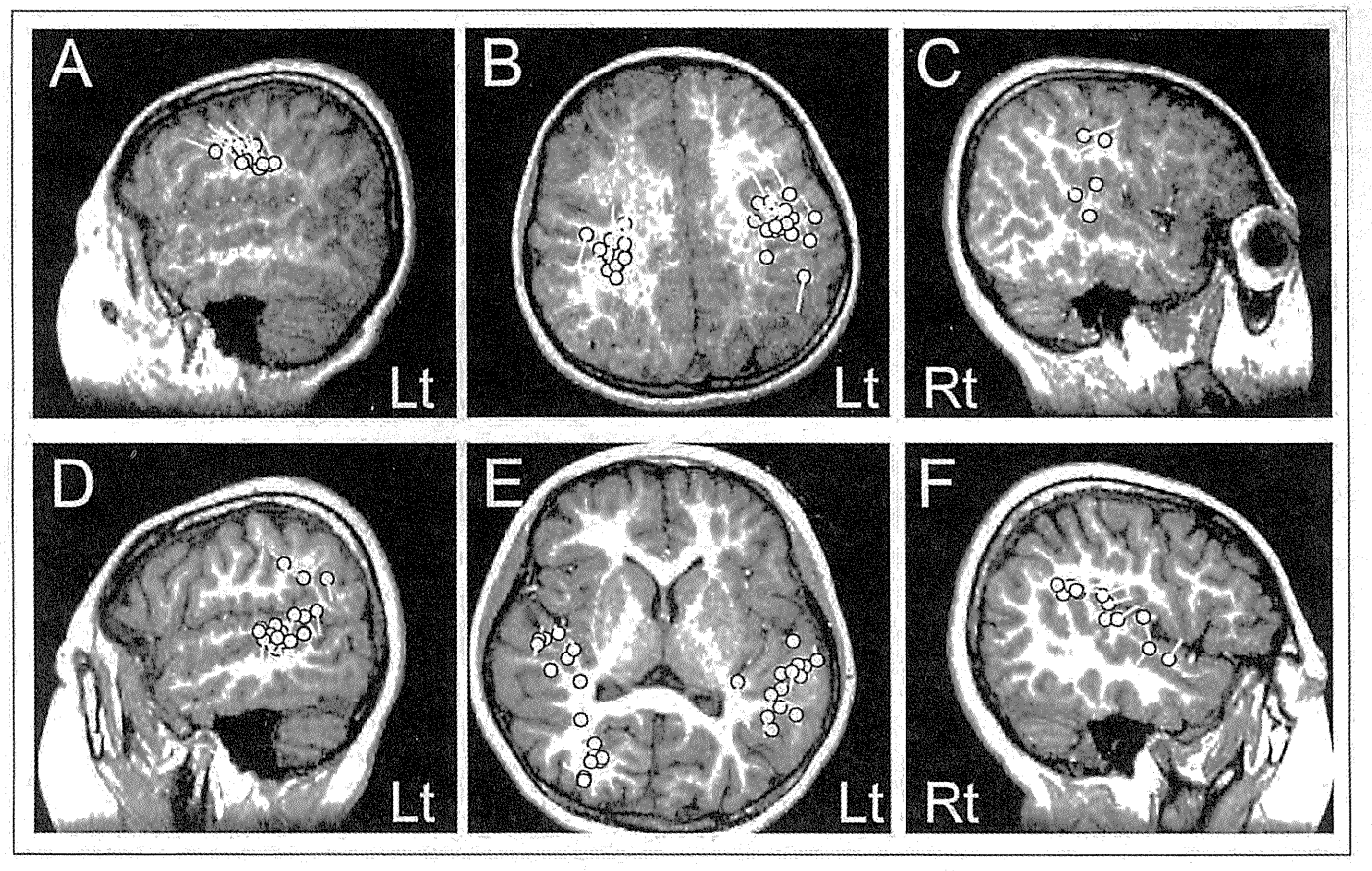

Figure 2. Figure shows magnetoencephalography images. All magnetic resonance imaging (MRI) is T1 weighted. Solid circles and tails represent locations and orientations of equivalent current dipoles for spike discharges. (A-C) Magnetic source images at age 7 years 7 months reveal clustering equivalent current dipoles of spike discharges in the prerolandic area of the left hemisphere, and around the central sulcus and sylvian fissure in the right hemisphere. (D-F) Magnetic source images at age 8 years 8 months reveal scattered equivalent current dipoles of spike discharges broadly surrounding the sylvian fissure, particularly on superior temporal gyri and sensory cortex of the left hemisphere, and superior temporal gyri and posterior temporal area of the right hemisphere. Abbreviations: Lt, left; Rt, right.

neurological deficit was not related to an ictal manifestation of epileptic seizures, but instead to epileptiform activity on EEG. They referred to paraictal cases presenting with opercular syndrome as having acquired opercular epilepsy. The present patient fits these criteria.

Landau-Kleffner syndrome is a rare epileptic disorder that is characterized by an acquired childhood aphasia associated with paroxysmal bi-temporal EEG abnormalities and auditory agnosia.[3] The reported EEG abnormalities in Landau-Kleffner syndrome are variable and heterogeneous. Several recent reports of magnetoencephalographic findings in Landau-Kleffner syndrome showed that the earliest spike activities were located in the superior temporal gyrus in the intrasylvian cortex. These results prompted the hypothesis that epileptiform activities cause dysfunction of the central auditory pathways and a deficit in the activation of the auditory cortical areas.[9,10] In contrast, acquired opercular epilepsy is a peculiar type of motor impairment associated with EEG abnormalities. The pathophysiological mechanism of this condition remains poorly understood. Shafrir and Prensky speculated that long-standing electrical dysfunction of perisylvian neurons causes bilateral neuronal dysfunction.[4] Tachikawa et al reported the results of computer-assisted electroencephalographic analysis in a patient with acquired opercular epilepsy, which demonstrated that all EEG foci were located in the left sylvian fissure and produced secondary bilateral synchronous sharp-slow complexes.[7] In previous magnetoencephalographic studies regarding typical benign rolandic epilepsy with centrotemporal spikes, the dipoles of rolandic spikes were tightly clustered in the sensorimotor cortex with constant anterior positivity in direction.[11,12] Kubota et al reported that magnetoencephalographic analysis in a patient with rolandic epilepsy and oromotor deficits demonstrated that current sources of rolandic discharges were broadly distributed in the secondary sensory cortex, superior temporal gyrus, and parietal association area in addition to the hand and orofacial divisions of the primary somatosensory cortex.[13] Our first magnetoencephalographic study demonstrated that the current sources of rolandic discharges were localized around the premotor area. This is compatible with the typical findings for atypical benign partial epilepsy with negative myoclonus.[14] On the second magnetoencephalographic study, the current sources of bilateral epileptic discharges were broadly distributed around the sylvian fissure, superior temporal gyrus, and sensory cortex. In addition, many of the current

discharges showed larger current magnitude than would be expected physiologically for a single spike, suggesting the simultaneous activation of a second source across a wide area. The present data and previous results indicated that the broadly distributed epileptic foci around the sylvian fissure including a secondary source cause specific prolonged neurological dysfunction observed in patients with acquired opercular epilepsy.

Although acquired opercular epilepsy is characterized by few epileptic seizures, proper treatment directed toward EEG abnormalities is likely to be necessary to improve neuropsychological impairment and motor deterioration. There is no standardized treatment for patients with epilepsy with a continuous spike and wave pattern, and several antiepileptics can be used. Benzodiazepines, such as clonazepam[7] and clobazam,[6] have resulted in dramatic improvements of clinical symptoms in patients with acquired opercular epilepsy. Moreover, combinations of various antiepileptic drugs and ketogenic diet were effective in a patient reported by Shafrir and Prensky.[4] In the present patient, epileptic seizures completely disappeared after clonazepam and ethosuximide were administered; however, neurocognitive and oromotor function deteriorated, and there was no electroencephalographic improvement. After initiating oral prednisolone, the symptoms improved dramatically, and EEG showed gradual improvement. Symptoms fluctuated as we tried to withdraw the prednisolone, so we continued low-dose prednisolone for more than 5 years without serious side effects. The effectiveness of oral corticosteroid therapy[15,16] and high-dose intravenous corticosteroid therapy[17] has been reported for language disorder in children with Landau-Kleffner syndrome. The possible mechanisms of action for corticosteroid remain unclear in electrical status epilepticus during sleep, but 1 hypothesis is an autoimmune reaction to central myelin in Landau-Kleffner syndrome.[18] On this basis, steroid and intravenous immunoglobulin have been used for the treatment of Landau-Kleffner syndrome.[19] The present case history suggests that prednisolone was also useful in the treatment of patients with intractable acquired opercular epilepsy without structural abnormalities.

The preferred mode of steroid administration is not yet clearly established, and we do not yet know the optimum dose and duration of prednisolone treatment for patients with Landau-Kleffner syndrome and acquired opercular epilepsy. Electrical status epilepticus during sleep is a heterogeneous disorder. To establish the appropriate treatments for the component disorders, further studies under appropriate epileptic conditions in the form of multicenter randomized controlled trails are necessary, because suitable cases are very rare.

Acknowledgments

We thank Ms Kuniko Tsuchiya and Mr Naoki Yamamoto for their excellent technical assistance.

Author Contributions

Jun Tohyama treated this patient in an outpatient clinic, analyzed magnetoencephalography, obtained financial support, and prepared this manuscript. Noriyuki Akasaka cared for this patient during hospitalization and performed adrenocorticotropic hormone, high-dose corticosteroid therapy, and oral corticisteroid therapy. Tsukasa Ohashi and Yu Kobayashi cared for this patient in outpatient clinic.

Declaration of Conflicting Interests

The authors declared no potential conflicts of interest with respect to the authorship and/or publication of this article.

Funding

The authors disclosed receipt of the following financial support for the research and/or authorship of this article: This study was supported in part by a Research Grant (20A-14) for Nervous and Mental Disorders from the Ministry of Health, Labor, and Welfare.

Ethical Approval

We obtained informed consent for publishing patient data and information from the patient and her parents.

References

1. Tassinari CA, Michelucci R, Forti A, et al. The electrical status epilepticus syndrome. In: Degen R, Dreifuss FE, eds. *Benign Localized and Generalized Epilepsies of Early Childhood.* Amsterdam: Elsevier; 1992;111-115.
2. Nickels K, Wirrell E. Electrical status epilepticus in sleep. *Semin Pediatr Neurol.* 2008;15:50-60.
3. Tassinari CA, Rubboli G, Volpi L, et al. Electrical status epilepticus during slow sleep (ESES or CSWS) including acquired epileptic aphasia (Landau-Kleffner syndrome). In: Roger J, Bureau M, Dravet Ch, et al., eds. *Epileptic Syndromes in Infancy, Childhood, and Adolescence.* 4th ed. Montrouge: John Libbey Eurotext; 2005; 295-314.
4. Shafrir Y, Prensky AL. Acquired epileptiform opercular syndrome: a second case report, review of the literature, and comparison to the Landau-Kleffner syndrome. *Epilepsia.* 1995;36: 1050-1057.
5. Roulet E, Deonna T, Despland PA. Prolonged intermittent drooling and oromotor dyspraxia in benign childhood epilepsy with centrotemporal spikes. *Epilepsia.* 1989:30:564-568.
6. de Saint-Martin A, Petiau C, Massa R, et al. Idiopathic rolandic epilepsy with "interictal" facial myoclonia and oromotor deficit: a longitudinal EEG and PET study. *Epilepsia.* 1999; 40:614-620.
7. Tachikawa E, Oguni H, Shirakawa S, et al. Acquired epileptiform opercular syndrome: a case report and results of single photon emission computed tomography and computer-assisted electroencephalographic analysis. *Brain Dev.* 2001;23:246-250.
8. Salas-Puig J, Pérez-Jiménez A, Thomas P, et al. Opercular epilepsies with oromotor dysfunction. In: Guerrini R, Aicardi J, Andermann F, Hallet M, eds. *Epilepsy and Movement Disorders.* Cambridge, MA: Cambridge University Press; 2002: 251-268.
9. Paetau R, Granström ML, Blomstedt G, et al. Magnetoencephalography in presurgical evaluation of children with the Landau-Kleffner syndrome. *Epilepsia.* 1999;40:326-335.

10. Sobel DF, Aung M, Otsubo H, Smith MC. Magnetoencephalography in children with Landau-Kleffner syndrome and acquired epileptic aphasia. *AJNR Am J Neuroradiol.* 2000;21:301-307.
11. Kamada K, Möller M, Saguer M, et al. Localization analysis of neuronal activities in benign rolandic epilepsy using magnetoencephalography. *J Neurol Sci.* 1998;154:164-172.
12. Ishitobi M, Nakasato N, Yamamoto K, Iinuma K. Opercular to interhemispheric source distribution of benign rolandic spikes of childhood. *NeuroImage.* 2005;25:417-423.
13. Kubota M, Takeshita K, Saitoh M, et al. Magnetoencephalographic analysis of rolandic discharges in a patient with rolandic epilepsy associated with oromotor deficits. *J Child Neurol.* 2004;19:456-459.
14. Kubota M, Nakura M, Hirose H, et al. A magnetoencephalographic study of negative myoclonus in a patient with atypical benign partial epilepsy. *Seizure.* 2005;14:28-32.
15. Marescaux C, Hirsch E, Finck S, et al. Landau-Kleffner syndrome: a pharmacologic study of five cases. *Epilepsia.* 1990;31:768-777.
16. Gallagher S, Weiss S, Cardy JO, et al. Efficacy of very high dose steroid treatment in a case of Landau-Kleffner syndrome. *Dev Med Child Neurol.* 2006;48:766-769.
17. Tsuru T, Mori M, Mizuguchi M, Momoi MY. Effects of high-dose intravenous corticosteroid therapy in Landau-Kleffner syndrome. *Pediatr Neurol.* 2000;22:145-147.
18. Nevšímalová S, Tauberová A, Doutlík S, et al. A role of autoimmunity in the etiopathogenesis of Landau-Kleffner syndrome? *Brain Dev.* 1992;14:342-345.
19. Mikati MA, Saab R. Successful use of intravenous immunoglobulin as initial monotherapy in Landau-Kleffner syndrome. *Epilepsia.* 2000;41:880-886.

CLINICAL REPORT

AMERICAN JOURNAL OF medical genetics PART A

Dandy–Walker Malformation Associated With Heterozygous *ZIC1* and *ZIC4* Deletion: Report of a New Patient

Jun Tohyama,[1,2]* Mitsuhiro Kato,[3] Sari Kawasaki,[4] Naoki Harada,[5] Hiroki Kawara,[5] Takeshi Matsui,[5] Noriyuki Akasaka,[1] Tsukasa Ohashi,[1] Yu Kobayashi,[1] and Naomichi Matsumoto[6]

[1]Department of Pediatrics, Nishi-Niigata Chuo National Hospital, Niigata, Japan

[2]Department of Pediatrics, Niigata University Medical and Dental Hospital, Niigata, Japan

[3]Department of Pediatrics, Yamagata University School of Medicine, Yamagata, Japan

[4]Department of Neurology, Saigata National Hospital, Jouetsu, Japan

[5]Department of Molecular Genetic Testing, Clinical Laboratory Center, Mitsubishi Chemical Medience Corporation, Nagasaki, Japan

[6]Department of Human Genetics, Yokohama City University Graduate School of Medicine, Yokohama, Japan

Received 10 February 2010; Accepted 9 July 2010

We report on a female patient with Dandy–Walker malformation possibly caused by heterozygous loss of *ZIC1* and *ZIC4*. The patient presented with mental retardation, epilepsy, and multiple congenital malformations including spina bifida, mild dysmorphic facial features including, thick eyebrows, broad nose, full lips, macroglossia, and hypoplasia of the cerebellar vermis with enlargement of the fourth ventricle on brain magnetic resonance imaging, which is consistent with Dandy–Walker malformation. A chromosome analysis showed interstitial deletion of chromosome 3q23-q25.1. Fluorescence in situ hybridization (FISH) and microarray-based genomic analysis revealed the heterozygous deletion of *ZIC1* and *ZIC4* loci on 3q24. Her facial features were not consistent with those observed in blepharophimosis–ptosis–epicanthus inversus syndrome (BPES) involving *FOXL2* abnormality. Other deleted genes at 3q23-25.1 might contribute to the dysmorphic facial appearance. A milder phenotype as the Dandy–Walker malformation in our patient supports the idea that modifying loci/genes can influence the development of cerebellar malformation.

Key words: Dandy–Walker malformation; interstitial deletion 3q; *ZIC1*; *ZIC4*

How to Cite this Article:
Tohyama J, Kato M, Kawasaki S, Harada N, Kawara H, Matsui T, Akasaka N, Ohashi T, Kobayashi Y, Matsumoto N. 2011. Dandy–Walker malformation associated with heterozygous *ZIC1* and *ZIC4* deletion: Report of a new patient.
Am J Med Genet Part A 155:130–133.

INTRODUCTION

Dandy–Walker malformation (DWM) is an abnormality in the development of the central nervous system that is defined by hypoplasia and upward rotation of the cerebellar vermis and cystic dilatation of the fourth ventricle [Hart et al., 1972; Parisi and Dobyns, 2003]. DWM is etiologically heterogeneous in association with a wide variety of chromosomal anomalies, various Mendelian disorders, multifactorial disorders, and environmental factors [Murray et al., 1985; Chitayat et al., 1994].

Grinberg et al. [2004] described seven nonrelated patients of DWM with de novo interstitial deletions of chromosome 3q. Cytogenetic investigation of these patients showed the first critical region involved in DWM, which encompasses genes *ZIC1* and *ZIC4*. There are five *Zic* genes encoding zinc finger proteins in humans and mice [Grinberg and Millen, 2005]. *ZIC1* and *ZIC4* are tightly linked on human chromosome 3 and mouse chromosome 9 [Grinberg et al., 2004; Grinberg and Millen, 2005]. A heterozygous deletion of these two linked genes in mice resulted in a phenotype that closely resembles DWM [Grinberg et al., 2004], strongly suggesting that heterozygous deletion of both *ZIC1* and *ZIC4* is the cause of DWM in humans. This is the second report on a new patient of DWM with heterozygous *ZIC1* and *ZIC4* deletion.

Grant sponsor: Ministry of Health, Labor and Welfare; Grant number: 20A-14.

*Correspondence to:
Jun Tohyama, M.D., Department of Pediatrics, Nishi-Niigata Chuo National Hospital, 1-14-1 Masago, Nishi-ku, Niigata 950-2085, Japan.
E-mail: jtohyama@masa.go.jp

Published online 10 December 2010 in Wiley Online Library (wileyonlinelibrary.com).
DOI 10.1002/ajmg.a.33652

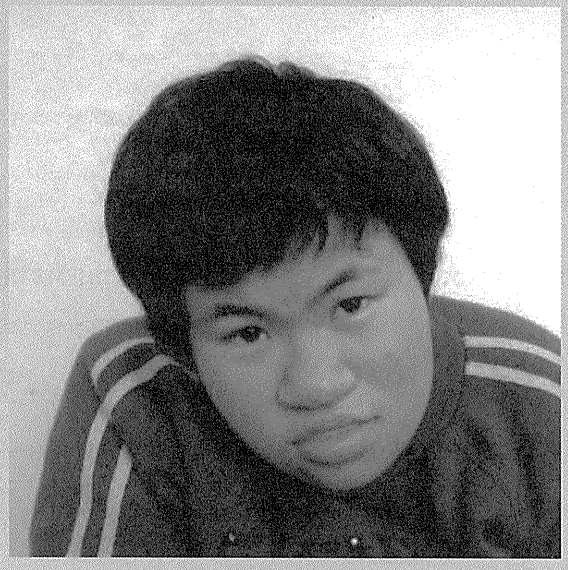

FIG. 1. Photograph of our patient at 21 years of age. Thick eyebrows, broad nose, and full lips are notable.

CLINICAL REPORT

A girl, the third child of healthy nonconsanguineous parents, was born at 41 weeks gestation by normal vaginal delivery following an uneventful pregnancy. Her elder brother has had epilepsy since age 10, however, his mental development was normal. Her birth weight was 2,880 g, length was 48 cm, and occipitofrontal circumference was 33 cm. A sacral dimple associated with occult spine bifida was found at birth. Computed tomography (CT) of the brain showed no sign of hydrocephalus. Follow-up CT at the age of 3 years showed mild dilatation of lateral ventricles. No treatment including surgical intervention was required at that time. Dislocation of both hip joints was also noted. After delivery, the patient received tube feeding for 3 months because of feeding difficulties and poor body weight gain. Her development was severely delayed: she could crawl by herself at age 1 year, and walk alone at 8 years. Hip joint dislocation was surgically repaired at 3 years. At 11 years, she developed generalized seizures, which were uncontrollable by various anti-epileptic drugs. On admission at 11 years, she showed dysmorphic features including thick eyebrows, a broad nose, full lips, and macroglossia, but no blepharophimosis/ptosis (Fig. 1). Mild scoliosis was also noted. Neurological examination revealed she had left hemiparesis with contracture of the lower and upper limbs. Both lower limbs were atrophic. Myoclonic movements on the left limbs were observed. Signs of cranial nerve impairment or cerebellar ataxia were evident. Electroencephalography identified a right-sided delta activity in the frontal lobe. Radiogram of facial bone showed no abnormal findings. Magnetic resonance imaging (MRI) of the brain showed hypoplasia and upward rotation of the cerebellar vermis and enlargement of the fourth ventricle, indicating DWM (Fig. 2A,B). The lateral ventricles were also enlarged. At 19 years, she could not speak. She could not walk alone because of deteriorating left hemiparesis with frequent seizures. She showed regular menstruation after menarche at 15 years.

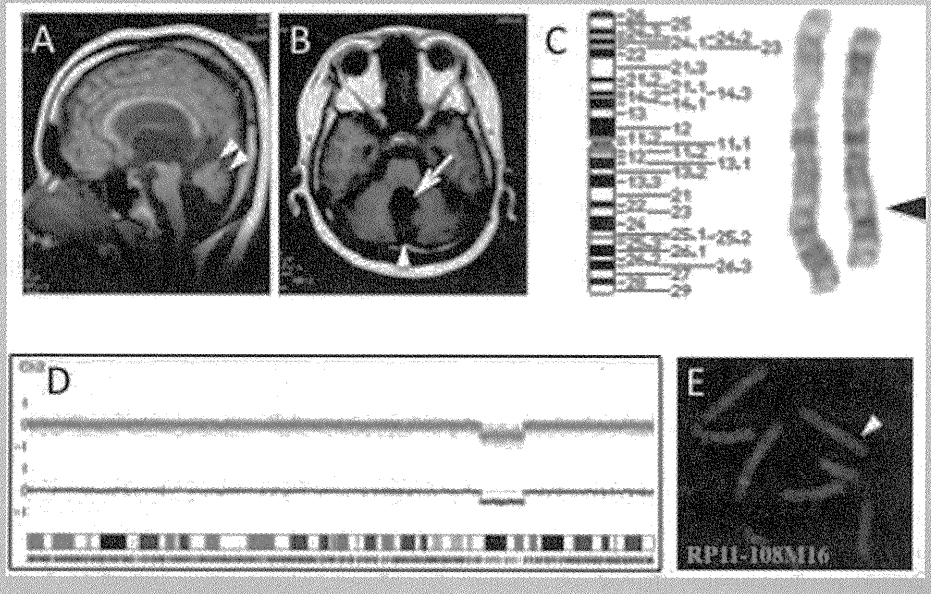

FIG. 2. A: Brain magnetic resonance imaging of the patient. Midline sagittal T1-weighted image shows hypoplasia and upward rotation of the cerebellar vermis (white arrowheads). B: Brain magnetic resonance imaging of the patient. Transverse T1-weighted image shows hypoplasia of the cerebellar hemisphere and vermis, and enlarged the fourth ventricle (white arrow). The fourth ventricle communicates with the posterior fossa fluid space (white arrowhead). C: Partial karyotype of the patient: del(3)(q23q25.1). The arrowhead indicates deletion. D: SNP chip analysis. A 14-Mb deletion is clearly demonstrated using CNAG 2.0 software. E: FISH analysis. RP11-108M16 covering *ZIC1* and *ZIC4* shows a heterozygous deletion (white arrowhead).

Cytogenetic and Genomic Analysis

Chromosomal analysis of her peripheral blood lymphocytes revealed that her karyotype was 46,XX,del(3)(q23q25.1) (Fig. 2C). Normal karyotype was confirmed in her parents. Her elder brother was not examined because abnormal features were not observed. To define chromosome 3q deletion, we performed genomic copy number analysis by GeneChip 250K Nsp Array (Affymetrix, Santa Clara, CA) and CNAG 2.0 software [Nannya et al., 2005] using the DNA of the patient's peripheral blood leukocytes. Copy number analysis clearly demonstrated the 14-Mb interstitial deletion: arr 3q23q25.31 (142,479,100–156,504,521) × 1 (Fig. 2D). According to the UCSC Genome Browser Human February 2009 Assembly, the deletion contains 67 RefSeq genes including following OMIM genes, *ATR*, *PLOD2*, *ZIC4*, *ZIC1*, *AGTR1*, *HPS3*, *CP*, *CLRN1*, *P2RY12*, and *MME*. Fluorescence in situ hybridization (FISH) using three BAC clones, RP11-108M16 (covering *ZIC4* and *ZIC1*), RP11-1001A3, and RP11-71N10 at 3q24, confirmed the deletion (Fig. 2E).

DISCUSSION

This patient presented with multiple congenital malformations, including occult spina bifida, dysmorphic facial features, and hypoplasia, and upward rotation of the cerebellar vermis with enlargement of the fourth ventricle on brain MRI, which were consistent with DWM. A cytogenetic analysis showed interstitial deletion of chromosome 3q23 to 3q25.1, and her FISH study confirmed the heterozygous deletion of *ZIC1* and *ZIC4* on 3q24. Recently, Grinberg et al. [2004] reported that locus 3q24 is the first critical region involved in DWM, encompassing genes *ZIC1* and *ZIC4*. The human ZIC gene family encoding zinc-finger transcription factors is comprised of five members [Grinberg and Millen, 2005]. The ZIC gene family is expressed in central nervous systems, including the cerebellum, and *Zic* genes are found to be expressed in the adult mouse cerebellum in a highly restricted manner [Aruga et al., 1994, 1996, 2002]. *Zic1* plays essential roles in cerebellar development, and the *Zic1* gene deletion could cause the extracerebellar phenotype as those reported in the *Zic1* knockout mice [Aruga et al., 1998; Ogura et al., 2001]. Human *ZIC1* and *ZIC4* are both mapped to 3p24. A mouse model for only $Zic1^{+/-}$ or $Zic4^{+/-}$ showed a slightly hypoplastic cerebellum, however, 15% of these double heterozygotes have severe cerebellar hypoplasia [Grinberg et al., 2004]. The authors conclude that heterozygous loss of *ZIC1* and *ZIC4* is the cause of DWM in individuals with deletion of 3q2. In our patient, we also demonstrated the heterozygous deletion of both *ZIC1* and *ZIC4* by FISH and SNP array. After the original report of seven cases, this is the second report dealing with the eighth case of DWM with heterozygous *ZIC1* and *ZIC4* deletion.

The original seven patients showed various phenotypes such as DWM. A wide variety of deletion in size was noted. The cerebellar hypoplasia in our patient is moderately severe as compared with those in the original seven cases. Chromosomal deletion in our patient ranges from 3q23 to 3q25.1. Grinberg et al. [2004] stated that the severity of DWM does not correlate with the size of chromosomal deletion. In the $Zic1^{+/-}$ $Zic4^{+/-}$ mice, 85% had a mild cerebellar phenotype whereas 15% were severely affected. The authors speculated that the variable expressivity observed in humans and mice might support the idea of modifying loci influencing the development of cerebellar malformation.

Three of the seven individuals in the report of Grinberg et al. [2004] have facial changes observed in the blepharophimosis–ptosis–epicanthus inversus syndrome (BPES), representing a recognizable contiguous gene syndrome [Smith et al., 1989; Ishikiriyama and Goto, 1993]. BPES is also an autosomal dominant inheritance and maps to 3q23 [Amati et al., 1995]. Crisponi et al. [2001] identified the forkhead transcription factor gene 2 (*FOXL2*) gene as responsible for BPES, which is located 3q22.3-q23. The facial dysmorphology of our patient is not consistent with BPES. To define her deletion, we performed a SNP array-based genomic copy number analysis and found that her interstitial deletion did not involve *FOXL2*. Only one of the five patients with 3q23-q25 deletion in the earlier reports showed no clinical features resembling BPES [Franceschini et al., 1983; Alvarado et al., 1987]. Dysmorphic facial features of this patient included synophrys of the eyebrows, broad nose, and full lips [Franceschini et al., 1983], partially resembling those of our case. Other deleted genes may affect the dysmorphic facial features in our patient.

DWM is a relatively common malformation of the central nervous system, but this condition has etiologic heterogeneity. After finding the first critical region of DWM, DeScipio et al. [2005] identified six children with subtelomeric deletions of 6p25, which is the second locus of DWM, and Aldinger et al. [2009] reported that the alteration of *FOXC1* at 6p25.3 contributed to DWM. In addition, Jalali et al. [2008] reported on a male patient with a heterozygous deletion of distal 2q, and identified a candidate locus for DWM with occipital cephalocele at 2q36.1 by linkage analysis. Their family showed an autosomal dominant mode of inheritance.

The recurrence risk for DWM is also heterogeneous, depending on the etiology, which is not yet fully explained despite intensive cytogenetic investigations of many cases. Empiric recurrence risk for DWM in the absence of a known disorder is relatively low [Murray et al., 1985]. High-resolution chromosomal analysis of patients may provide critical information necessary for genetic counseling related to DWM.

ACKNOWLEDGMENTS

The authors thank Dr. Masashi Suda and Dr. Shigeru Maruyama for providing patient information. This study was supported in part by a Research Grant (20A-14) for Nervous and Mental Disorders from the Ministry of Health, Labor and Welfare.

REFERENCES

Aldinger KA, Lehmann OJ, Hudgins L, Chizhikov VV, Bassuk AG, Ades LC, Krantz ID, Dobyns WB, Millen KJ. 2009. *FOXC1* is required for normal cerebellar development and is a major contributor to chromosome 6p25.3 Dandy–Walker malformation. Nat Genet 41:1037–1042.

Alvarado M, Bocian M, Walker AP. 1987. Interstitial deletion of the long arm of chromosome 3: Case report, review, and definition of a phenotype. Am J Med Genet 27:781–786.

Amati P, Chomel JC, Nivelon-Chevalier A, Gilgenkrantz S, Kitzis A, Kaplan J, Bonneau D. 1995. A gene for blepharophimosis-ptosis-epicanthus inversus syndrome maps to chromosome 3q23. Hum Genet 96:213–215.

Aruga J, Yokota N, Hashimoto M, Furuichi T, Fukuda M, Mikoshiba K. 1994. A novel zinc finger protein, Zic, is involved in neurogenesis, especially in the cell lineage of cerebellar granule cells. J Neurochem 63:1880–1890.

Aruga J, Nagai T, Tokuyama T, Hayashizaki Y, Okazaki Y, Chapman VM, Mikoshiba K. 1996. The mouse *Zic* gene family. Homologues of the *Drosophila* pair-rule gene *odd-paired*. J Biol Chem 271:1043–1047.

Aruga J, Minowa O, Yaginuma H, Kuno J, Nagai T, Noda T, Mikoshiba K. 1998. Mouse *Zic1* is involved in cerebellar development. J Neurosci 18:284–293.

Aruga J, Tohmonda T, Homma S, Mikoshiba K. 2002. Zic1 promotes the expansion of dorsal neural progenitors in spinal cord by inhibiting neuronal differentiation. Dev Biol 244:329–341.

Chitayat D, Moore L, Del Bigio MR, MacGregor D, Ben-Zeev B, Hodgkinson K, Deck J, Stothers T, Ritchie S, Toi A. 1994. Familial Dandy–Walker malformation associated with macrocephaly, facial anomalies, developmental delay, and brain stem dysgenesis: Prenatal diagnosis and postnatal outcome in brothers. A new syndrome? Am J Med Genet 52:406–415.

Crisponi L, Deiana M, Loi A, Chiappe F, Uda M, Amati P, Bisceglia L, Zelante L, Nagaraja R, Porcu S, Ristaldi MS, Marzella R, Rocchi M, Nicolino M, Lienhardt-Roussie A, Nivelon A, Verloes A, Schlessinger D, Gasparini P, Bonneau D, Cao A, Pilia G. 2001. The putative forkhead transcription factor *FOXL2* is mutated in blepharophimosis/ptosis/epicanthus inversus syndrome. Nat Genet 27:159–166.

DeScipio C, Schneider L, Young TL, Wasserman N, Yaeger D, Lu F, Wheeler PG, Williams MS, Bason L, Jukofsky L, Menon A, Geschwindt R, Chudley AE, Saraiva J, Schinzel AAGL, Guichet A, Dobyns WE, Toutain A, Spinner NB, Krantz ID. 2005. Subtelomeric deletions of chromosome 6p: Molecular and cytogenetic characterization of three new cases with phenotypic overlap with Ritscher-Shinzel (3C) syndrome. Am J Med Genet Part A 134A:3–11.

Franceschini P, Silengo MC, Davi G, Bianco R, Biagioli M. 1983. Interstitial deletion of the long arm of chromosome 3 in a patient with mental retardation and congenital anomalies. Hum Genet 64:97.

Grinberg I, Millen KJ. 2005. The *ZIC* gene family in development and disease. Clin Genet 67:290–296.

Grinberg I, Northrup H, Ardinger H, Prasad C, Dobyns WB, Millen KJ. 2004. Heterozygous deletion of the linked genes *ZIC1* and *ZIC 4* is involved in Dandy–Walker malformation. Nat Genet 36: 1053–1055.

Hart MN, Malamud N, Ellis WG. 1972. The Dandy–Walker syndrome. A clinicopathological study based on 28 cases. Neurology 22:771–780.

Ishikiriyama S, Goto M. 1993. Blepharophimosis sequence (BPES) and microcephaly in a girl with del(3)(q22.2q23): A putative gene responsible for microcephaly close to the BPES gene? Am J Med Genet 47: 487–489.

Jalali A, Aldinger KA, Chary A, Mclone DG, Bowman RM, Le LC, Jardine P, Newbury-Ecob R, Mallick A, Jafari N, Russell EJ, Curran J, Nguyen P, Ouahchi K, Lee C, Dobyns WB, Millen KJ, Pina-Neto JM, Kessler JA, Bassuk AG. 2008. Linkage to chromosome 2q36.1 in autosomal dominant Dandy–Walker malformation with occipital cephalocele and evidence for genetic heterogeneity. Hum Genet 123:237–245.

Murray JC, Johnson JA, Bird TD. 1985. Dandy–Walker malformation: etiologic heterogeneity and empiric recurrence risks. Clin Genet 28: 272–283.

Nannya Y, Sanada M, Nakazaki K, Hosoya N, Wang L, Hangaishi A, Kurokawa M, Chiba S, Bailey DK, Kennedy GC, Ogawa S. 2005. A robust algorithm for copy number detection using high-density oligonucleotide single nucleotide polymorphism genotyping arrays. Cancer Res 65: 6071–6079.

Ogura H, Aruga J, Mikoshiba K. 2001. Behavioral abnormalities of *Zic1* and *Zic2* mutant mice: implications as models for human neurological disorders. Behav Genet 31:317–324.

Parisi MA, Dobyns WB. 2003. Human malformations of the midbrain and hindbrain: review and proposed classification scheme. Mol Genet Metab 80:36–53.

Smith A, Fraser IS, Shearman RP, Russell P. 1989. Blepharophimosis plus ovarian failure: a likely candidate for a contiguous gene syndrome. J Med Genet 26:434–438.

Pediatric Neurology 45 (2011) 193–196

Contents lists available at ScienceDirect

Pediatric Neurology

journal homepage: www.elsevier.com/locate/pnu

Case Report

Hemiconvulsion-Hemiplegia-Epilepsy Syndrome Associated With *CACNA1A* S218L Mutation

Sawako Yamazaki MD [a,*], Kanju Ikeno MD [a], Tokinari Abe MD [a], Jun Tohyama MD [b], Yoshiki Adachi MD [c]

[a] *Department of Pediatrics, Niigata City General Hospital, Niigata, Japan*
[b] *Department of Pediatrics, Nishi-Niigata Chuo National Hospital, Niigata, Japan*
[c] *Department of Neurology, Matsue Medical Center, Matsue, Japan*

ARTICLE INFORMATION

Article history:
Received 16 December 2010
Accepted 18 April 2011

ABSTRACT

Hemiconvulsion-hemiplegia-epilepsy syndrome involves sudden and prolonged unilateral seizures, followed by transient or permanent hemiplegia and epilepsy during infancy or early childhood. Some patients with familial hemiplegic migraine and demonstrating the S218L mutation in *CACNA1A* experience severe attacks with unilateral cerebral edema after trivial head trauma. We report on a 5-year-old Japanese girl presenting with hemiconvulsion-hemiplegia-epilepsy syndrome after infection with parvovirus B19. Magnetic resonance imaging performed 2 days after admission revealed cerebellar atrophy and marked hyperintensity in the left hemisphere on T_2-weighted and diffusion-weighted imaging. Magnetic resonance angiography performed 7 days after admission demonstrated obliteration of the left proximal middle cerebral artery in the acute phase. However, this finding was not evident on brain angiography performed 25 hours after magnetic resonance angiography. Genetic analysis of familial hemiplegic migraine revealed a heterozygous S218L mutation in *CACNA1A*. Taken together, these results suggest that vasospasms of cerebral vascular smooth muscle, with possible cortical spreading depression, may have caused the hemiconvulsions and hemiplegia in the left hemisphere. This case report is the first, to the best of our knowledge, to associate *CACNA1A* with hemiconvulsion-hemiplegia-epilepsy syndrome and familial hemiplegic migraine, and to suggest that similar pathogenic mechanisms may underlie these two disorders.

Introduction

Hemiconvulsion-hemiplegia-epilepsy syndrome is a rare condition involving sudden and prolonged unilateral seizures in infancy and early childhood, followed by transient or permanent hemiplegia. Eighty percent of patients subsequently develop focal epilepsy. The clinical features, natural history, and neuroradiologic findings were studied extensively [1,2], but the pathogenesis remains poorly understood.

Familial hemiplegic migraine is a rare autosomal dominant subtype of migraine with aura in which attacks are associated with hemiparesis and, in some families, cerebellar atrophy [3,4]. Three genes, *CACNA1A* at chromosome 19p13, *ATP1A2* at 1q23, and *SCNA1A* at 2q24, were identified to cause type 1, type 2, and type 3 familial hemiplegic migraine, respectively. Each of these genes encodes proteins involved in ion transportation [4,5]. Some patients with familial hemiplegic migraine and manifesting the S218L mutation in *CACNA1A* were reported to experience severe attacks with unilateral cerebral edema after trivial head trauma [6-8]. This mutation tends to cause severe and specific phenotypes, such as familial hemiplegic migraine [9].

We report on a 5-year-old Japanese girl with hemiconvulsion-hemiplegia-epilepsy syndrome after infection with parvovirus B19, who manifested the S218L mutation in *CACNA1A*.

Case Report

A 5-year-old Japanese girl had been born without asphyxia. She presented with a documented history of delayed motor and mental development and cerebellar ataxia from infancy. No other members of her immediate family reported a history of severe headache. Cranial magnetic resonance imaging at age 11 months indicated no abnormalities. At both 3 years and 6 months and 4 years and 5 months of age, she experienced episodes of unconsciousness for more than 2 hours after vomiting. Interictal electroencephalography revealed no abnormal findings. At age 5 years and 3 months, she developed erythema infectiosum. Ten days after the onset of infection, vomiting and complex partial seizures began, accompanied by right

* Communications should be addressed to: Dr. Yamazaki; Department of Pediatrics; Niigata City General Hospital; 463-7 Syumoku; Chuo-ku , Niigata 950-1197, Japan.
E-mail address: yy.sawako@luck.ocn.ne.jp

0887-8994/$ - see front matter © 2011 Elsevier Inc. All rights reserved.
doi:10.1016/j.pediatrneurol.2011.04.010

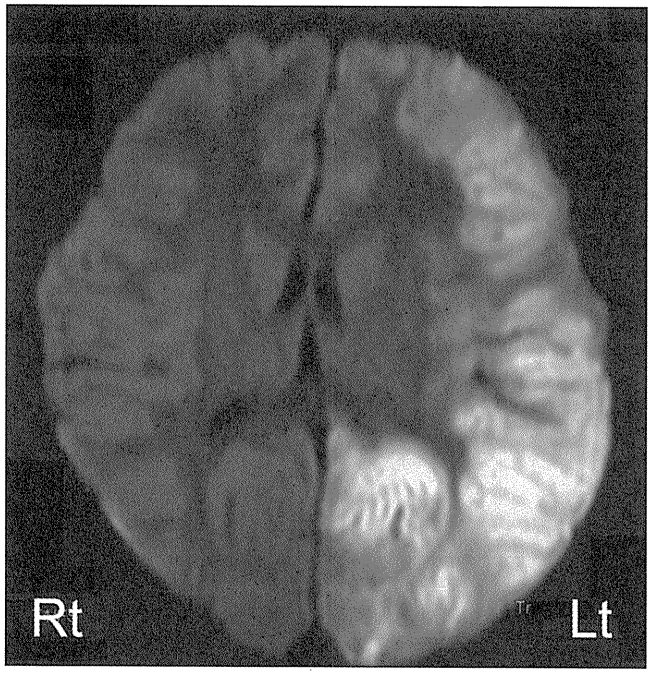

Figure 1. Cranial magnetic resonance imaging 2 days after onset of infection, at age 5 years and 3 months. Axial diffusion-weighted imaging indicates hyperintensity of the white matter in the left cerebral hemisphere, predominantly involving subcortical white matter. Lt = left; Rt = right.

hemiconvulsions for more than 1 hour. When she arrived at our hospital, her seizures continued. An intravenous injection of midazolam was administered, and she recovered from the complex partial status epilepticus. Six hours after admission, she manifested a high fever. The day after admission, she was incapable of speech and of voluntary movements in the right limbs. Serum amino acid analysis, urine organic acid analysis, and cerebrospinal fluid examination yielded normal results. Her level of serum anti-parvovirus B19 immunoglobulin M antibody was elevated, and a polymerase chain reaction analysis of serum detected parvovirus B19 DNA. Cranial magnetic resonance imaging performed 2 days after admission revealed cerebellar atrophy and widespread areas of mild hyperintensity on T_2-weighted images and marked hyperintensity on diffusion-weighted images, revealing lesions (Fig 1) in the cortex and subcortical white matter of the left frontal, temporal, and parietal lobes. Follow-up magnetic resonance imaging performed 7 days after admission demonstrated an expansion of brain edema in the left cerebral hemisphere, compared with T_2-weighted imaging from the previous magnetic resonance image. Magnetic resonance angiography performed 7 days after admission demonstrated an obliteration of the left proximal middle cerebral artery (Fig 2A), but no such obliteration was evident on brain angiography performed 8 days after admission (Fig 2B). Five days after admission, she manifested several episodes of right hemiconvulsions lasting for 5-6 minutes. Oral administration of carbamazepine and clobazam was initiated, and her seizures were controlled. She was discharged 45 days after admission, with right hemiparesis and mild dysarthria. A third cranial magnetic resonance image performed 90 days after the onset of infection indicated diffuse atrophy of the left cerebral hemisphere (Fig 3).

Clinically, hemiconvulsion-hemiplegia-epilepsy syndrome associated with parvovirus B19 infection was diagnosed. Suspecting a relationship between hemiconvulsion-hemiplegia-epilepsy syndrome and familial hemiplegic migraine, we used the polymerase chain reaction direct sequencing method to sequence exons 4, 5, 6, 17, 26, 27, 28, and 32 of *CACNA1A*, and exons 17 and 19 of *ATP1A2*, where many mutations have accumulated. DNA was extracted from peripheral blood using a standard protocol. We identified the heterozygous S218L mutation in exon 5 of *CACNA1A*.

Discussion

Our patient developed prolonged complex partial seizures with right hemiconvulsions, high fever, and right hemiparesis after infection with parvovirus B19. Cranial magnetic resonance imaging revealed marked hyperintensity in the left hemisphere on diffusion-weighted imaging during the acute stage. Right hemiconvulsions were later evident, and severe atrophy of the left cerebral hemisphere was apparent on magnetic resonance imaging during the chronic phase. Hemiconvulsion-hemiplegia-epilepsy syndrome after infection with parvovirus B19 was thus diagnosed. The clinical picture of this patient did not present the usual signs of familial hemiplegic migraine attacks. However, because of her history of cerebellar ataxia and episodic unconsciousness with vomiting, we hypothesized that her signs may have been related to hemiplegic migraine, and we performed genetic testing for familial hemiplegic migraine. We were then able to identify the S218L mutation in *CACNA1A*. To the best of our knowledge, this report is the first to associate the mutation in *CACNA1A* with hemiconvulsion-hemiplegia-epilepsy syndrome.

The pathogenesis of hemiconvulsion-hemiplegia-epilepsy syndrome has been widely discussed, but has yet to be fully explained [1,2,10]. Involvement of a primary viral infection with human herpesvirus 7, Varicella zoster virus, and the other viruses were reported [11,12]. These data cannot explain why unilateral lesions resulted. Kawada et al. suggested that a cerebrovascular disorder attributable to human herpesvirus 7 infection may constitute the cause of hemiconvulsion-hemiplegia-epilepsy syndrome [11]. The lesions of hemiconvulsion-hemiplegia-epilepsy syndrome may also represent a direct consequence of prolonged, unilateral febrile convulsions [1,13]. Results from our patient could provide important insights into the pathogenesis of hemiconvulsion-hemiplegia-epilepsy syndrome.

Kors et al. [6] first reported the S218L mutation in *CACNA1A* in association with familial hemiplegic migraine. The S218L mutation is one of the more common in familial hemiplegic migraine type 1, and patients with this mutation are known to suffer from particularly severe attacks, accompanied by cerebral edema [6-8]. Stem et al. [8] summarized the clinical spectrum in 13 patients with the S218L mutation. They reported that 12 patients (92%) manifested ataxia or cerebellar signs, and nine patients (69%) manifested hemiplegic migraine that may have triggered by trivial head trauma. In addition, nine patients (69%) exhibited severe attacks with coma. In our patient, because no head trauma was recognized before her attack, hemiconvulsions with impaired consciousness may have been triggered by infection with parvovirus B19, and she demonstrated unilateral effects of her infection in the brain. These results strongly suggest that the pathogenesis of hemiconvulsion-hemiplegia-epilepsy syndrome may partially overlap those of familial hemiplegic migraine. The mechanism of the migraine aura is considered to be associated with the cortical spreading depression induced by a dysfunction of neuronal voltage-dependent P/Q-type calcium channels. Accompanying the S218L mutation, P/Q-type calcium channels exhibit an unusually low threshold of activation, a very slow rate of inactivation, and a fast rate of recovery from inactivation [4,5,9]. This effect of the S218L mutation may contribute to hemiconvulsion-hemiplegia-epilepsy syndrome.

We performed cerebral angiography during the acute stage. In a previous report, severe episodes in patients with familial hemiplegic migraine were triggered by cerebral angiography [14]. In our patient, no worsening of signs was evident after angiography. Some reports described cranial angiography in addition to the findings of magnetic resonance angiography in cases of familial hemiplegic migraine attacks. Our patient demonstrated an obliteration of the left proximal middle cerebral artery on magnetic resonance angiography just after her attack, but this finding was not evident on brain angiography the next day. We postulated that the obliteration of the left proximal middle cerebral artery on magnetic resonance angiography did not indicate mechanical obstruction, but vasospasms of this artery instead. Involvement of the entire left hemisphere in our patient could not be explained only by ischemic

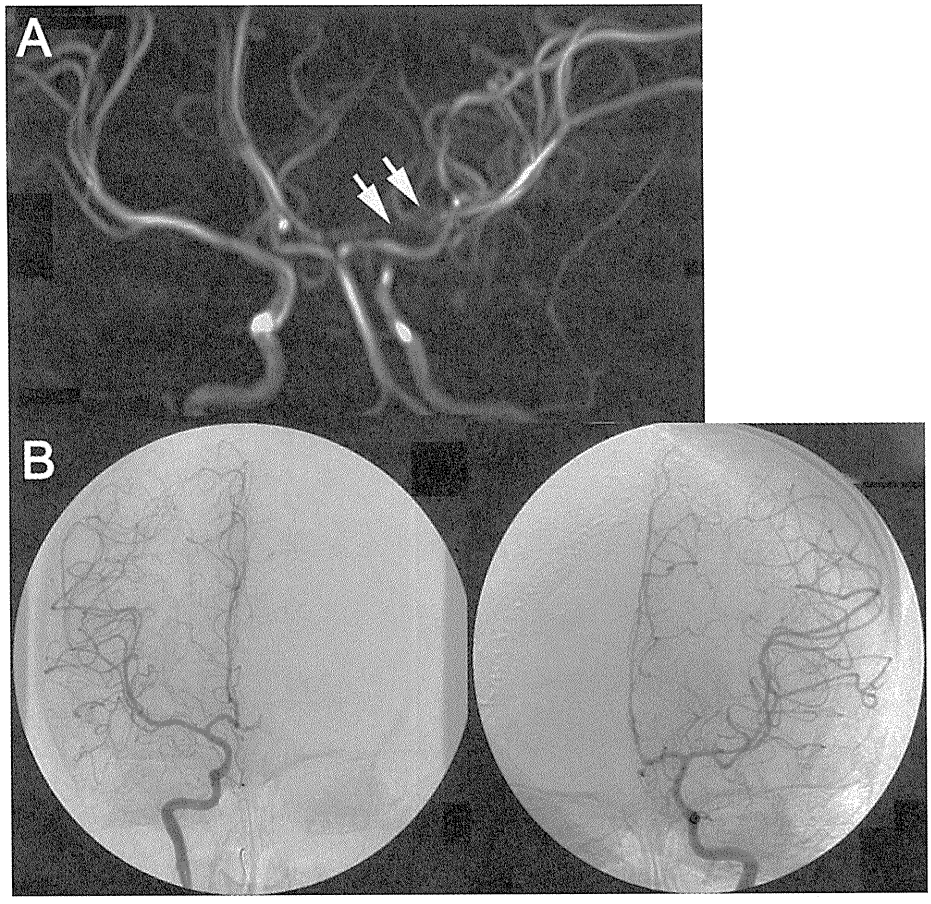

Figure 2. Findings of angiography. (A) Cranial magnetic resonance angiography 7 days after onset of infection, at age 5 years and 3 months, demonstrates obliteration of the left proximal middle cerebral artery (arrows). (B) Cranial angiography of the right carotid artery (left) and left carotid artery (right) at 8 days after onset of infection indicates a patent left middle cerebral artery.

changes in the middle cerebral artery area. We think that vasospasms of the cerebral vascular smooth muscle, attributable to channel impairment with cortical spreading depression, may have caused the hemiconvulsions and hemiplegia.

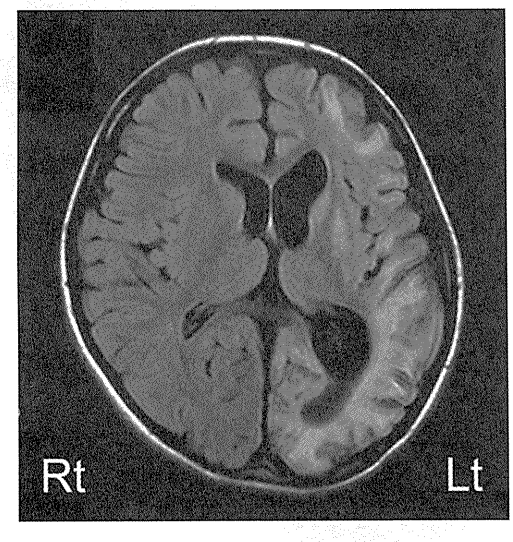

Figure 3. Cranial magnetic resonance imaging at 90 days after onset of infection. Axial fluid-attenuated inversion recovery image indicates diffuse atrophy of the left cerebral hemisphere. Lt = left; Rt = right.

In conclusion, this report is the first, to the best of our knowledge, of a *CACNA1A* S218L mutation in a patient with hemiconvulsion-hemiplegia-epilepsy syndrome. Further analyses of the *CACNA1A* gene in a larger number of patients with hemiconvulsion-hemiplegia-epilepsy syndrome may provide more evidence of relationships between hemiconvulsion-hemiplegia-epilepsy syndrome and familial hemiplegic migraine, and confirm whether similar pathogenic mechanisms underlie these two disorders, and how often this gene may be involved.

The authors thank the doctors of neurosurgery and the staff at the Department of Radiology of Niigata City General Hospital for performing emergency brain angiography, and the doctors of radiology and neurology at Niigata City General Hospital for helpful suggestions.

References

[1] Freeman JL, Coleman LT, Smith LJ, Shield LK. Hemiconvulsion-hemiplegia-epilepsy syndrome: Characteristic early magnetic resonance imaging findings. J Child Neurol 2002;17:10–6.
[2] Mirsattari SM, Wilde NJ, Pigott SE. Long-term cognitive outcome of hemiconvulsion-hemiplegia-epilepsy syndrome affecting the left cerebral hemisphere. Epilepsy Behav 2008;13:678–80.
[3] Headache Classification Committee of the International Headache Society. The international classification of headache disorders, 2nd edition. Cephalalgia 2004;24(Suppl. 1):1–160.
[4] Pietrobon D. Familial hemiplegic migraine. Neurotherapeutics 2007;4:274–84.
[5] Ophoff RA, Terwindt GM, Vergouwe MN, et al. Familial hemiplegic migraine and episodic ataxia type-2 are caused by mutations in the Ca^{2+} channel gene CACNL1A4. Cell 1996;87:543–52.

[6] Kors EE, Terwindt GM, Vermeulen FLMG, et al. Delayed cerebral edema and fatal coma after minor head trauma: Role of the CACNA1A calcium channel subunit gene and relationship with familial hemiplegic migraine. Ann Neurol 2001;49:753–60.
[7] Curtain RP, Smith RL, Ovcaric M, Griffiths LR. Minor head trauma-induced sporadic hemiplegic migraine coma. Pediatr Neurol 2006;34: 329–32.
[8] Stam AH, Luijckx GJ, Poll-Thé BT, et al. Early seizures and cerebral oedema after trivial head trauma associated with the *CACNA1A* S218L mutation. J Neurol Neurosurg Psychiatry 2009;80:1125–9.
[9] Debiais S, Hommet C, Bonnaud I, et al. The FHM1 mutation S218L: A severe clinical phenotype? A case report and review of the literature. Cephalalgia 2009;29:1337–9.
[10] Toldo I, Calderone M, Boniver C, Dravet C, Guerrini R, Laverda AM. Hemiconvulsion-hemiplegia-epilepsy syndrome: Early magnetic resonance imaging findings and neuroradiological follow-up. Brain Dev 2007;29: 109–11.
[11] Kawada J, Kimura H, Yoshikawa T, et al. Hemiconvulsion-hemiplegia-epilepsy syndrome and primary human herpesvirus 7 infection. Brain Dev 2004;26:412–4.
[12] Wakamoto H, Ohta M, Nakano N. Hypercytokinemia in hemiconvulsions-hemiplegia-epilepsy syndrome associated with dual infection with Varicella zoster viruses and Epstein-Barr virus. Neuropediatrics 2002;33: 262–5.
[13] Hisano T, Ohno M, Egawa T, Takano T, Shimada M. Changes in diffusion-weighted MRI after status epilepticus. Pediatr Neurol 2000;22: 327–9.
[14] Ducros A, Denier C, Joutel A, et al. The clinical spectrum of familial hemiplegic migraine associated with mutations in a neuronal calcium channel. N Engl J Med 2001;345:17–24.

Progressive Atrophy of the Cerebrum in 2 Japanese Sisters with Microcephaly with Simplified Gyri and Enlarged Extraaxial Space

Authors: M. Hirose[1], K. Haginoya[1,2], H. Yokoyama[3], A. Kikuchi[1], N. Hino-Fukuyo[1], M. Munakata[1], M. Uematsu[1], K. Iinuma[4], M. Kato[5], T. Yamamoto[6], S. Tsuchiya[1]

Affiliations: Affiliation addresses are listed at the end of the article

Key words
- microcephaly
- simplified gyri
- enlarged extraaxial space
- atrophy

Abstract

This is a case report that describes 2 sisters with microcephaly, simplified gyri, and enlarged extraaxial space. Clinical features of the cases include dysmorphic features, congenital microcephaly, failure of postnatal brain growth, neonatal onset of seizures, quadriplegia, and severe psychomotor delay. Neuroradiological imaging demonstrated hypoplasia of bilateral cerebral hemispheres with enlarged extraaxial spaces, simplified gyral patterns without a thickened cortex, hypoplastic corpus callosum, and enlarged lateral ventricles, with a reduction in gray and white matter volume during the prenatal and neonatal periods. Repeat MRI revealed progressive atrophy of the cerebral gray and white matter, with enlarged lateral ventricles, although the sizes of the bilateral basal ganglia, thalamus, and infratentorial structures were relatively preserved. These neuroradiological findings imply that this disease is caused by the gene involved in neuronal and glial proliferation in the ventricular zone and in tangential neuronal migration from the ganglionic eminence. The nature of the progressive degeneration of the hemispheric structures should be clarified.

Introduction

From medical records and brain images in 237 patients with brain malformations characterized as microcephaly with simplified gyri, Basel-Vanagaite and Dobyns classified patients into 4 major groups: microcephaly with simplified gyri only, microcephaly with simplified gyri and pontocerebeller hypoplasia, microcephaly with simplified gyri and enlarged extraaxial space, and microcephaly with simplified gyri and both pontocerebeller hypoplasia and enlarged extraaxial space [1]. One of these groups, microcephaly with simplified gyri and enlarged extraaxial space is clinically characterized by severe developmental failure, feeding difficulty, spastic quadriplegia, and dyskinesia, with postnatal or congenital brain growth failure [occipital frontal circumference (OFC) below − 3 SD]. MRI findings typically show microcephaly, simplified gyri, enlarged extraaxial space and relatively preserved pontocerebeller structures [1]. In this case study, we describe 2 Japanese sisters with microcephaly with simplified gyri and enlarged extraaxial space. In one of the sisters, repeat MRI findings showed progressive atrophy of the cerebral hemispheres.

Case Report

Patient 1

The older sister, the first child of unrelated parents, was born after 38 weeks gestation by spontaneous delivery following a normal pregnancy. Microcephaly was noted during fetal ultrasonographic examination in the last trimester. The patient's birth weight was 2400 g (−1.5 SD), length 45.0 cm (−1.7 SD), and OFC 30 cm (−2.2 SD). She temporally showed clonic seizure activity on day 0. Upon admission at the age of 1 month, her general condition was unremarkable in spite of microcephaly and feeding difficulties. Dysmorphic features including a sloping forehead, arched and thick eyebrows, blephalophimosis, a saddle nose, triangular mouth, and micrognathia were observed. She began having complex partial seizures with right facial clonic seizures at 2 months of age. The seizures were controlled with valproic acid. The patient had spastic quadriplegia without obvious spontaneous movements and gastroesophageal reflux disease (GERD) beginning at 3 months of age. She died suddenly at 4 years and 8 months of age.

received 25.04.2011
accepted 28.08.2011

Bibliography
DOI http://dx.doi.org/10.1055/s-0031-1287771
Neuropediatrics 2011; 42: 163–166

ISSN 0174-304X

Correspondence
Kazuhiro Haginoya, MD, PhD
Department of Pediatric Neurology
Takuto Rehabilitation Center for Children
20 Shikaoto
Akiu Yumoto
Taihaku-ku
Sendai 982-0241
Japan
Tel.: +81/22/398 2221
Fax: +81/22/397 2697
khaginoya@silk.ocn.ne.jp